Motion State Recognition of Debris Ejected in Vehicular Collision after Contact with the Ground

Xuejing Du*[1], Daizhong Su[2] and Zhanyu Wang[1]
[1]Transportation College, Northeast Forestry University, China
[2]Advanced Design and Manufacturing Engineering Centre, School of Architecture, Design and the Built Environment, Nottingham Trent University, UK
E-mail: duxuejing99@163.com, daizhong.su@ntu.ac.uk, zywang77@163.com
*Corresponding author

Abstract: The motion state of debris ejected from the vehicle involved in vehicular collision is important for finding-out the vehicle collision speed. This research developed an analytical model to recognize the debris motion state. With the model, analyses were conducted, which reveal that if α, which is the contact angle between the debris and the ground at the moment when the debris collides the ground, is within the range from 0° to its boundary value, then the debris slides; if α is within the range from its boundary value to 90°, then the debris bounces. With debris' initial angular velocity ω =0, the boundary value is 11.8° for sphere debris and 7.8° for rectangular debris; with $\omega \neq 0$, the boundary value for rectangular debris is $\arcsin\frac{g}{R\omega^2}$ where g represents the acceleration due to gravity and R is the distance from the debris centre to the point of its contact with the ground. Experiment tests were conducted for debris motion states with ω =0, which confirmed the analytical results.
Keywords: vehicle engineering; vehicular collision; collision debris; motion state; recognition mode.

Biographical notes: Xuejing Du is an associate professor and has been working in Vehicle Engineering Department of Transportation College, Northeast Forestry University, China since 2008. She received her PhD degree in transportation engineering from Jilin University, China in 2008. Her current research involves traffic environment, vehicle collision and safety technology, and light weight design of automobile. Her research has been supported by funding from various sources including the National Natural Science Foundation of China (NSFC), Natural Science Foundation of Heilongjiang Province of China, Higher Education Funds of Heilongjiang Province of China, International Cooperation of Northeast Forestry University, Transport Research of Heilongjiang Province of China, and Fundamental Research Funds of the Central Universities. She also participated in the collaborative projects sponsored by Volkswagen and the Development and Reform Commission of Jilin Province.

Daizhong Su is Professor of Design Engineering and leads the Advanced Design and Manufacturing Engineering Centre at Nottingham Trent University, UK. His research interests include machine and mechanisms, environment protection and sustainability, integrated design and manufacturing, and condition monitoring. His research has been supported by grants from various founding organisations including European Commission, UK research funding bodies, Royal Society, industries and international organisations. He is editor in chief of the International Journal of Design Engineering published by Inderscience. He has been involved in organising more than 20 international conferences as Conference Chair, Co-chair, international chair and committee members. He has about 220 refereed research publications.

Zhanyu Wang is an associate professor and has been working at the Northeast Forestry University, China since 2009. He received his PhD degree in 2009. The major areas of his research and teaching include vehicle collision and safety technology, traffic

pollution and environment protection, and automobile theory/technology and simulation. His recent research is supported by the grant from the Natural Science Foundation of Heilongjiang Province, China.

1 Introduction

Vehicle collision often happens in traffic accidents. In order to understand the nature of the vehicular collision and to determine the responsibility of each party involved in the accident, it is important to find out the vehicle impact speed at the moment of a collision. In the accident scene, there are usually a large amount of debris ejected from the vehicle involved in the collision, and the debris can be used to recognize the collision impact speed, because the vehicle debris moves at a velocity related to the velocity of the vehicle just prior to impact. As such, the distance with which vehicle debris travels at a traffic accident scene is an important parameter for calculating collision velocity of the vehicle. However, once ejected debris makes contact with the ground following a vehicular collision, it could have several possible motion states such as bouncing, sliding, sticking, and rolling-sliding. The different motion states lead to different travel distances for an equivalent initial velocity. Therefore, the motion state of the debris plays an important role in determining the vehicle speeds at the moment of the collision.

When relative tangential velocity exists at the contact point in a collision between the debris and the ground, friction will affect the collision process. Coulomb friction theory has been conventionally employed to estimate the influence of friction in the collision process, but the motion state of debris cannot be determined after the collision, because Coulomb friction theory is invalid under certain conditions (Peter and Hu, 2003). Brach (1984) deduced the typical equation representative of oblique impact by applying a restitution coefficient and an equivalent friction coefficient. Keller (1986) took the limited duration of impact into account to calculate the direction of impact friction of two rigid bodies in the process of collision. Yigit (1990) pointed out that the restitution coefficient was proportional to the relative impact velocity. Thornton (1997) defined the restitution coefficient as an explicit expression of the yield velocity and the relative impact velocity. Hayakawa (2002) determined the motion state of debris in two ways, one was determined by applying the relationship between the dynamic friction coefficient and the critical friction coefficient, the other was determined by the relationship between ratios involving the normal velocity and tangential velocity of debris before and after a collision with the ground and the friction coefficient. Hamid (2001) used Routh's graphical method to establish a general formulation of impact in the conditions of compression and restitution phases. Yao (2005, 2007) obtained a solution to changes in the energy restitution coefficient according to the initial conditions by analyzing the friction collision problem comprehensively in a multi-body system. Xu (2008) established a collision dynamics equation.

However, all the equations/methods discussed above do not consider the motion state of debris after making contact with the ground. The fact that the travel distance of debris differs depending on the motion state after contact with the ground is essential for accurate accident reconstruction. Du (2012) and Xu (2013) made progress in a mathematical model of the debris travel distance for accident reconstruction. Meanwhile, Du (2013) and Niea (2014) made efforts to reconstruct and investigate the accidents involving pedestrian and bicycle. Socia (2016) took into account ten parameters, such as road inclination, friction coefficient between the pedestrian and the ground, vehicle and pedestrian mass, and pedestrian launch angle to analyze the collision phase. Then, an alternative model was presented to determine the pedestrian thrown distance. Both pedestrian and bicycle are also called debris in accident scene defined by the public security industry standards (2005). However, these existing researches still have not

considered the effect of the motion states of debris on the travel distance.

Happer (2000) and Toor (2003) investigated the vehicle's collision with pedestrians, which considered the pedestrian's rolling, sliding and rolling-sliding states after the vehicle collided the pedestrian; however, the boundary values were not given, and, hence, the methods are not applicable in actual calculation.

To obtain an accurate debris travel distance equation for conducting accident reconstruction and to find out the vehicle impact speed, it is necessary to establish the conditions determining different motion states of debris after contact with the ground. Hence, the present study applies the contact state assessment method for rigid bodies employed in modern contact dynamics to determine the motion states of debris after contact with the ground. As revealed in the literature review presented above, there has not been a proper analytical model for the debris motion states. The research presented in this paper fills this gap with the analytical model developed, which is a novel contribution in recognition of motion states of debris in vehicular collision and helps to understand the nature of the vehicular collision and to determine the responsibility of each party involved in the accident.

In the following sections, after description of the problem involved in determination of motion states of vehicle debris in a vehicle collision, the analytical model of debris motion states is established first, and then analyses are carried out using the model developed. With the analysis results, the motion states can be determined. To validate the analytical results, experiments were conducted for the motion states of sphere and rectangular debris pieces within contact range 0°~90°. The concluding remarks and future work are given in the final section.

2 Problem description and the analytical model of debris motion states

Owing to the complexity of friction coefficient, the motion state of debris is very difficult to determine after the debris colides with the ground. Based on the contact state assessment method for rigid bodies employed in modern contact dynamics (Peter and Hu, 2003; Glcocker and Pfeiffer, 2001), an analytical model is developed in this research, which includes the equations, primary and supplementary criteria, and principles to determine the motion states of debris after contact with the ground, based on the contact angle between the debris and the ground, as detailed in this section.

2.1 Problem description and related equations

Fig. 1 illustrates the states of debris pre-and-post contact with the ground, where $C(x,y)$ is the center of mass coordinates of debris, R is the distance from $C(x,y)$ to the point of contact, g is the acceleration due to gravity, g_N is the distance from the lowest point of the debris to the ground, α is the angle between the ground and R (i.e., the contact angle), m is the mass and mg is the gravitation of debris, F_t is the tangential force of contact, and F_n is the normal force.

Figure 1 States of debris pre-and-post contact with the ground (R, F_t, F_n are scalar quantities.).

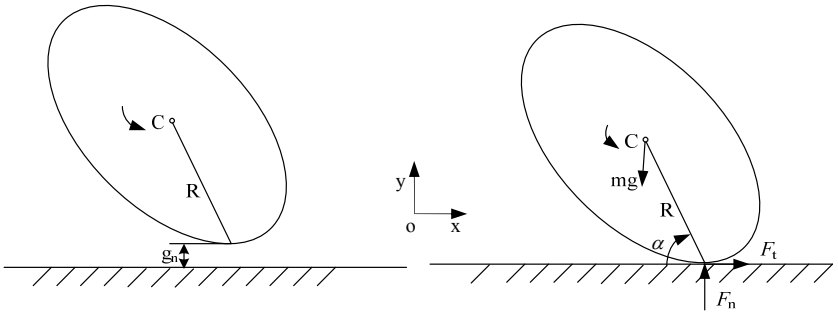

At the moment of contact with the ground, the variable g_N is established as the parameter determining whether debris collides with the ground. The transient motion can be given as follows.

$$\begin{cases} m\ddot{x} = F_t \\ m\ddot{y} = F_n - mg \\ I_s\ddot{\alpha} = -F_n R\cos\alpha - F_t R\sin\alpha \end{cases} \tag{1}$$

where $(\ddot{x},\ddot{y})$ is the coordinates' center of mass acceleration of the debris, and I_s is its rotational inertia. The value of I_s varies with the shape of the debris, which can be calculated as follows.

$$I_s = mk^2, \tag{2}$$

where k is the rotational radius of the debris.

We establish the initial normal and tangential displacements of the debris at the moment of contact, denoted respectively as g_N and g_T, based on the following expressions.

$$\begin{cases} g_T = x + R\cos\alpha \\ g_N = y - R\sin\alpha \end{cases} \tag{3}$$

where x and y are the initial displacements of $C(x,y)$.

The relative normal and tangential accelerations of the contact point can be obtained as follows.

$$\begin{cases} \ddot{g}_N = \ddot{y} - R\ddot{\alpha}\cos\alpha + R\dot{\alpha}^2\sin\alpha \\ \ddot{g}_T = \ddot{x} - R\ddot{\alpha}\sin\alpha - R\dot{\alpha}^2\cos\alpha \end{cases} \tag{4}$$

where, $\ddot{x}$ and $\ddot{y}$ are the tangential and normal accelerations of $C(x,y)$, respectively, and $\ddot{\alpha}$ is the angular acceleration of $C(x,y)$. Substitute Eqs. (1) and (3) into Eq. (4) yields the following.

$$\begin{cases} \ddot{g}_N = \dfrac{1}{m}[1 + \dfrac{R^2}{k^2}\cos\alpha(\cos\alpha + \mu\sin\alpha)]F_n + (R\dot{\alpha}^2\sin\alpha - g) \\ \ddot{g}_T = \dfrac{1}{m}[\mu + \dfrac{R^2}{k^2}\sin\alpha(\cos\alpha + \mu\sin\alpha)]F_n - R\dot{\alpha}^2\cos\alpha \end{cases} \tag{5}$$

where, μ is frictional coefficient between debris and ground.

2.2 **The criteria for determination of the debris motion states**

By combining the terms given in Eq. (5), we can define a **primary criterion** regarding debris contact:

$$\ddot{g}_N = AF_n + B \,. \tag{6}$$

where, $A = \frac{1}{m}[1 + \cos\alpha(\cos\alpha + \mu\sin\alpha)]$, $B = R\dot{\alpha}^2 \sin\alpha - g$.

Then, a **supplementary criterion** for the motion state of contacting debris is given as

$$\ddot{g}_N \geq 0, F_n \geq 0; \ddot{g}_N \cdot F_n = 0 \,. \tag{7}$$

When $F_n = 0, \ddot{g}_N \geq 0$, debris is in a state of non-contact with the ground; however, when $F_n \geq 0, \ddot{g}_N = 0$, the debris is in contact with the ground.

According to the criterion established through Eqs. (6) and (7), the motion states of debris can be categorized according to the value of A, which could have three cases: $A > 0$, $A < 0$, or $A=0$.

For $B= 0$, there could be two instances: either $F_n = 0$, then $\ddot{g}_N = 0$; or $\ddot{g}_N = 0$, then $F_n = 0$. However, both instances are impossible, because $F_n = 0$ and $\ddot{g}_N = 0$ means that the debris does not contact with the ground, and stays in the air without movement, which does not exist according to the supplementary criterion mentioned above. Therefore, only $B > 0$ and $B < 0$ are considered below, without consideration of $B= 0$.

2.3. **Determination of the debris motion states**

Based on the analysis in section 2.1, the principles are given below for determination of the debris motion states, which are based on three cases: A > 0, A < 0, or A=0, and, in each case, only $B > 0$ and $B < 0$ are considered.

(1) Determination of debris motion stats in the case $A > 0$.

For $B > 0$, if $F_n = 0$, then $\ddot{g}_N = B > 0$, the debris will bounce after contacting the ground. However, if $\ddot{g}_N = 0$, then $F_n = -\frac{B}{A} < 0$, which is not satisfied with supplementary criterion expressed in Eq. (7) that $F_n \geq 0$, making this assumption invalid.

For $B < 0$, if $F_n = 0$, then $\ddot{g}_N = B > 0$. However, it is inconsistent with the assumption that $B < 0$; hence, the assumption is invalid. If $F_n > 0$ and $\ddot{g}_N = 0$, $F_n = -\frac{B}{A} > 0$, then debris will slide after making contact with the ground.

(2) Determination of debris motion states in the case $A < 0$.

For $B > 0$, if $F_n = 0$, then $\ddot{g}_N = B > 0$ or $\ddot{g}_N = 0$, and $F_n = -\frac{B}{A} > 0$, making the two assumptions valid. The debris will be rolling-sliding after making contact with the ground.

For $B < 0$, if $F_n = 0$, then $\ddot{g}_N = B < 0$ or $\ddot{g}_N = 0$, and $F_n = -\frac{B}{A} < 0$, and the two conditions are inconsistent with the previous assumption. Hence, both assumptions are invalid.

(3) Determination of the debris motion state in the case $A = 0$.

For $B > 0$, if $F_n = 0$, then $\ddot{g}_N = B \geq 0$; if $\ddot{g}_N = 0$, then $F_n = -\frac{B}{A} = \infty$. However, it is inconsistent with $A= 0$, making this assumption invalid.

For $B < 0$, if $F_n = 0$, then $\ddot{g}_N = B < 0$. However, it is inconsistent with supplementary criterion for the debris motion states that $\ddot{g}_N \geq 0, F_n \geq 0; \ddot{g}_N \cdot F_n = 0$, making this assumptions invalid.

Therefore, $A = 0$ is invalid for determination of the debris motion states, and, hence,

$A = 0$ is not considered in the following analysis.

3 The theoretical analysis results

3.1 Motion state recognition of spherical debris

For spherical debris, $k = R$ in Eq. (5), which yields the following.

$$\begin{cases} \ddot{g}_N = \dfrac{1}{m}[1+\cos\alpha(\cos\alpha+\mu\sin\alpha)]F_n + (R\dot{\alpha}^2\sin\alpha - g) \\ \ddot{g}_T = \dfrac{1}{m}[\mu+\sin\alpha(\cos\alpha+\mu\sin\alpha)]F_n - R\dot{\alpha}^2\cos\alpha \end{cases} \tag{8}$$

Here, A and B are defined as follows:

$A = \dfrac{1}{m}[1+\cos\alpha(\cos\alpha+\mu\sin\alpha)]$, $B = R\dot{\alpha}^2\sin\alpha - g$.

The following three contact conditions can be obtained for spherical debris according to the primary criterion and supplementary criterion:

(1) If $A > 0$ and $B > 0$, $F_n = 0$, and then $\ddot{g}_N = B > 0$. Spherical debris will bounce after making contact with the ground.

(2) If $A > 0$ and $B < 0$, $\ddot{g}_N = 0$, and then $F_n = -\dfrac{B}{A} > 0$. Spherical debris will slide after making contact with the ground.

(3) If $A < 0$ and $B > 0$, $F_n = 0$, and then either $\ddot{g}_N = B > 0$ or $\ddot{g}_N = 0$, and $F_n = -\dfrac{B}{A} > 0$, making both assumptions invalid. Hence, spherical debris will be in a state of rolling-sliding after making contact with the ground.

Figure 2 Linear complementarity problem (LCP) diagram for spherical debris

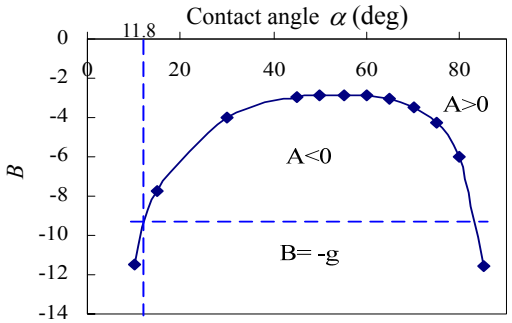

Fig. 2 presents the linear complementarity problem (LCP) diagram corresponding to the motion state of spherical debris according to the primary criterion and supplementary criterion of debris under the condition of no initial angular velocity ω=0. The results shown in Fig. 2 are obtained by solving equations (7) and (8) using the numerical iterative approximation method. Based on the LCP diagram results, the motion state of spherical debris can be determined under the given condition as a function of α, as follows.

If α is within the range from 0° to 11.8°, spherical debris will slide to a stop after

making contact with the ground.

If α is within the range from 11.8° to 90°, spherical debris will bounce after making contact with the ground.

3.2 Motion state recognition of rectangular debris

Rigid rectangular debris of side lengths a and b and center of mass o in free fall exhibit the four types of motion states illustrated in Fig. 3, which are dictated by air resistance and surface friction conditions. Debris in states (a) and (b) will not rotate, but slide only. However, debris in states (c) and (d) will rotate or bounce owing to the effect of surface friction，which are in contact called point impact. The type of borderline condition is satisfied by the relative speed of rectangular debris, which will determine its motion state.

Figure 3 Rigid rectangular debris making contact with the ground

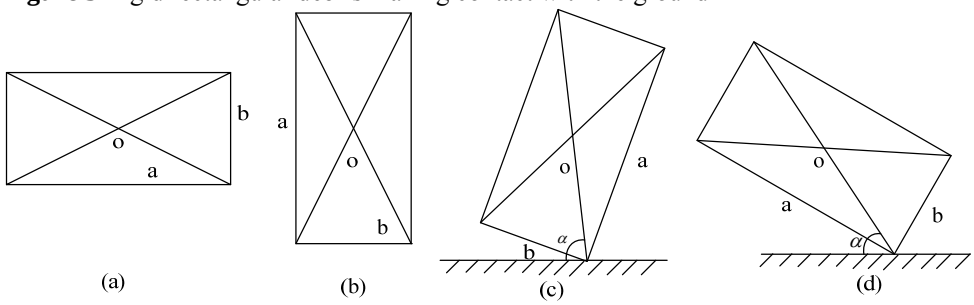

Fig. 4 and Fig. 5 respectively show the state of motion of rectangle debris prior to contact with the ground and the force conditions at the moment of contact.

Figure 4 State of motion for rectangular debris prior to contact

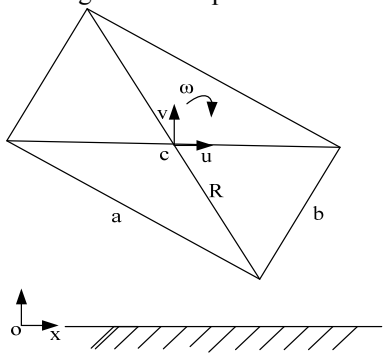

Figure 5 Force conditions for rectangular debris at the moment of contact

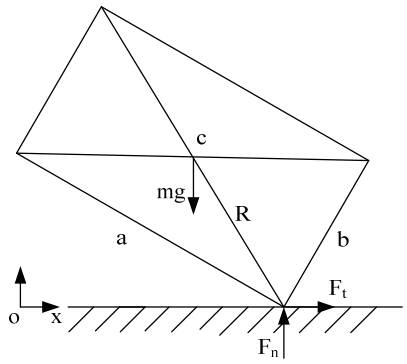

For rectangular debris, $k=\frac{R}{\sqrt{3}}$, for $R=\frac{\sqrt{a^2+b^2}}{2}$ in Eq. (5), which yields the following.

$$\begin{cases}\ddot{g}_N=\frac{1}{m}[1+3\cos\alpha(\cos\alpha+\mu\sin\alpha)]F_n+(R\dot{\alpha}^2\sin\alpha-g)\\ \ddot{g}_T=\frac{1}{m}[\mu+3\sin\alpha(\cos\alpha+\mu\sin\alpha)]F_n-R\dot{\alpha}^2\cos\alpha\end{cases} \tag{9}$$

Here, A and B are defined as follows:

$A=\frac{1}{m}[1+3\cos\alpha(\cos\alpha+\mu\sin\alpha)]$; $B=R\dot{\alpha}^2\sin\alpha-g$.

The following three contact conditions for rectangular debris can be obtained according to the primary criterion and supplementary criterion.

(1) If $A>0$ and $B>0$, $F_n=0$, and then $\ddot{g}_N=B>0$. Rectangular debris will bounce after making contact with the ground.

(2) If $A>0$ and $B<0$, $\ddot{g}_N=0$, and then $F_n=-\frac{B}{A}>0$. Rectangular debris will slide after making contact with the ground.

(3) If $A<0$ and $B>0$, $F_n=0$, and then either $\ddot{g}_N=B>0$ or $\ddot{g}_N=0$, and $F_n=-\frac{B}{A}>0$, making both assumptions valid. Hence, the motion state of rectangular debris will be rolling-sliding after making contact with the ground.

LCP diagrams for rectangular debris can be obtained according to the primary criterion and supplementary criterion, as shown in Fig. 6 for conditions of $\omega=0$, and Fig. 7 under conditions of $\omega\neq 0$. The results shown in Fig. 6 and Fig. 7 are obtained by solving equations (7) and (9) using the numerical iterative approximation method. The motion state of rectangular debris for $\omega=0$ can be determined based on the LCP diagram results as shown in Fig. 6.

Figure 6 LCP diagram of rectangular debris with no initial angular velocity

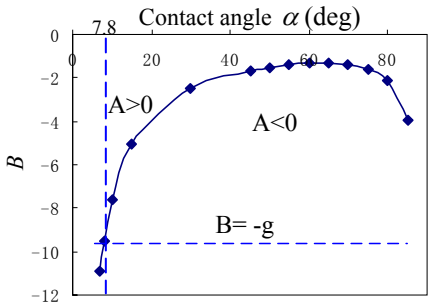

If α is within the range from 0° to 7.8°, rectangular debris will slide after making contact with the ground.

If α is within the range from 7.8° to 90°, rectangular debris will bounce after making contact with the ground.

The motion state of rectangular debris with an initial value of $\omega \neq 0$ can be determined based on the LCP diagram results as shown in Fig. 7.

Figure 7 LCP diagram of rectangular debris with an initial angular velocity ω

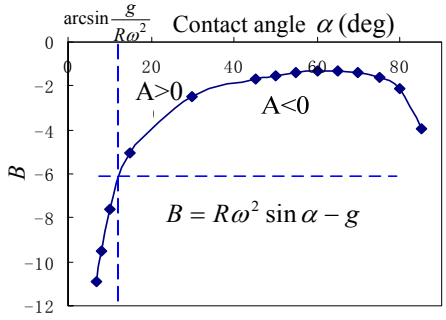

If α is within the range from 0° to $\arcsin\frac{g}{R\omega^2}$, rectangular debris will slide after making contact with the ground.

If α is within the range from $\arcsin\frac{g}{R\omega^2}$ to 90°, rectangular debris will bounce after making contact with the ground.

4 Experimental validation

4.1 The experimental test system

In order to validate the theoretical analysis results, a debris motion state test system has been developed and built by this research. The test system is shown in Fig. 8, which comprised of an object ejection device (Fig. 9), of which the ejection angle can be adjusted; a high speed camera (Fig. 10); and video recording equipment (Sony VCR and CCD monitor; Fig. 11) for monitoring and recording the contact angle and the motion state of the ejected debris onto both VHS cassette and computer for subsequent analyses, as well as leveling instrument, spotlights, and a protractor.

Figure 8 The motion state test system

Figure 9 The ejection device

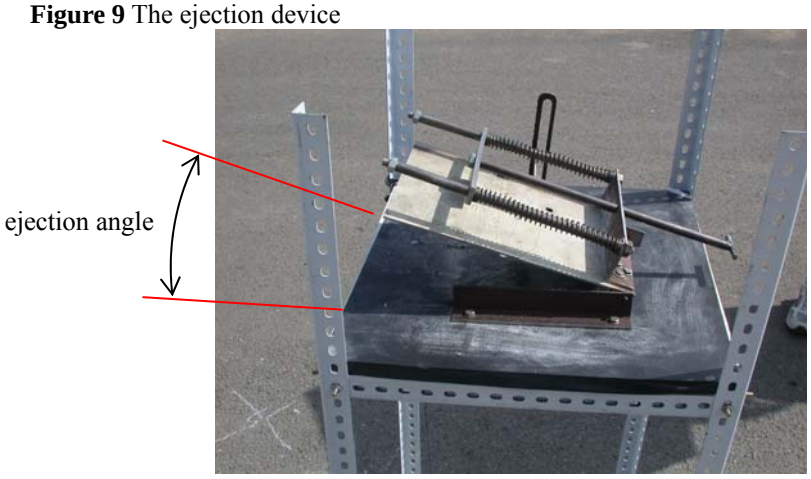

Figure 10 High-speed camera

Figure 11 CCD monitor and Sony VCR

The expected debris contact angle α with the ground at the contact point is obtained by adjusting the ejection angle of the ejection device shown in Fig. 9, because the change of ejection angle results in the change of contact angle. The ejection angle can be adjusted within the range from 0° to 90°. An ejection force is exerted on an object by a spring, and the force can be calculated according to the measured speed at contact with the ground. The ejection force depends on the stiffness H of the selected spring, and the object velocity v is related to m and the extent of spring compression X according to the following equations.

$$\frac{1}{2}mv^2 = \frac{1}{2}HX^2; v = \sqrt{\frac{H}{m}}X \tag{10}$$

A parallel-double spring ejection device was adopted, the stiffness of which can be obtained as

$$H = \sum_{i=1}^{2} H_i = 2\frac{Gd^4}{8nD_2^3} = \frac{Gd^4}{4nD_2^3}, \tag{11}$$

where, G is the shear modulus, d is the spring diameter, n is the number of active coils, and D is outer diameter of coil.

4.2 Experimental test

Different sized spherical debris and rectangular debris were taken as test objects. The tests were conducted for various values of α with $\omega = 0$. The contact angle between the debris and the ground, as well as the motion states of the debris after it contacts the ground, are recorded by the High-speed camera，CCD monitor，Sony VCR，and the data are then processed by the computer. The test results are listed in Table 1, which reveal the following:

- For the sphere debris, if the contacting angle α within the range 0° ~11.8°, the debris slides till it stops, while α is over 7.8°, the debris bounces till it stops.
- For the rectangular debris, if the contacting angle α within the range 0° ~7.8°, the debris slides till it stops, while α is over 11.8°, the debris bounces till it stops.

The above results confirm the theoretical analysis results obtained in Section 3.1 for the sphere debris and in Section 3.2 for rectangular debris.

Table 1 Motion state of debris

Debris \ Contact angle	0°	3.9°	7.8°	11.8°	27.4°	43°	58.7°	74.4°	90°
Spherical	slide	slide	slide	slide	bounce	bounce	bounce	bounce	bounce
Rectangular	slide	slide	slide	bounce	bounce	bounce	bounce	bounce	bounce

5 Conclusions

In order to understand the nature of the vehicular collision and to determine the responsibility of each parties involved in the accident, it is important to find out the vehicle impact speed at the moment of the collision. The motion state of debris ejected from the vehicle involved in the collision affects the accuracy of the collision impact speed calculation. However, in the existing methods of calculating the collision speed, the motion states of vehicle debris have not been considered, because there has not been an applicable analytical model for the debris motion states. To fill this gap, this research developed the analytical model for recognizing the debris motion states and conducted relevant experimental validation, which made novel contribution to knowledge in the subject area.

In this research, the analytical model is developed by applying contact dynamics and LCP graphic method, which can be used to recognize the motion states of the vehicle debris during a vehicular collision. The motion states covered by the analytical model include bouncing, sliding and rolling-sliding. The sticking state is easy to be recognized, so it is not necessary to consider it in the analytical model.

With the model, the analyses and calculations were conducted for confirmation of the debris motion states. There is a boundary value of contact angle α to determine the debris motion state: if α is within the rage from 0° to the boundary value, then the debris slides, and if α is within the rage from the boundary value to 90°, the debris bounces. In the situation that the debris' initial angular velocity ω=0, the boundary value is 11.8° for sphere debris and 7.8° for rectangular debris; in the situation that the rectangular debris with initial angle velocity $\omega \neq 0$, the boundary value is $\arcsin\frac{g}{R\omega^2}$.

This research also developed an experimental test system, with which experiments were conducted for the motion states of sphere and rectangular debris pieces with α in the range 0°~90°. The experimental results validated the theoretical analysis results.

For motion state of debris with $\omega \neq 0$, this research conducted analytical investigation of rectangular debris only, but sphere debris has not be investigated. As part of the future research, the analytical model of motion state for sphere debris with $\omega \neq 0$ will be developed, and corresponding analytical results will be provided.

Due to the limitation in obtaining the debris' angular velocity and difficulty to develop the experimental devices, the experimental test for motion stats of debris with $\omega \neq 0$ has not been done in the current research. This will be conducted as future research work, including both sphere and rectangular debris. In addition, experimental investigations for rolling-sliding motion state will be conducted.

Acknowledgement

The research reported in his paper is supported by the National Natural Science

Foundation of China (Grant No. 51108068), Natural Science Foundation of Heilongjiang province (Grant No. E201350), and the S&T Plan Projects of Heilongjiang Provincial Education Department (Grant No. 11553025).

References

A. S. Yigit, A. G. Ulsoy and R. A. Scott. (1990) 'Dynamics of a radially rotating beam with impact, part 1: theoretical and computational model', *Journal of Vibration and Acoustics*, Vol. 112, pp.65- 70.

A. soica. S. Tarulescu. (2016) 'Impact phase in frontal vehicle-pedestrian collisions', *International Journal of Automotive Technology*, Vol.17, pp. 387-397

C. Thornton. (1997) 'Coefficient of restitution for collinear collisions of elastic-perfectly plastic spheres', *Journal of Applied Mechanics*, Vol. 64, pp. 383-386.

DU Xue-jing, XU Hong-guo, WANG Zhan-yu. (2012) 'Generalized kinetic behavior model of debris in vehicle collision', *Highlights of Science paper Online*, Vol. 5, pp.1185-1191.

Glcocker, CH. Pfeiffer, F.(2001) *'Mutiple Contact Problems in Multibody Dynamics a Review*'. Kluwer Academic Publishers, Netherlands

H. Hayakawa and H. Kuninaka. (2002) 'Simulation and theory of the impact of two-dimensional elastic disks', *Chemical Engineering Science*, Vol. 57, pp.239-252.

H. M. Lankarani and M. F. O. S. Pereira. (2001) 'treatment of impact with friction in planar multibody mechanical systems', *Multibody System Dynamics*, Vol. 6, pp. 203-227.

Happer, A., Araszewski, M., Toor, A., Overgaard, Johal, R. (2000) 'Comprehensive Analysis Method for Vehicle/Pedestrian Collisions'. *SAE*, paper 2000-01-0846.

Hart Peter, JiBin Hu. (2003) *Modern contact dynamics*, Southeast University press, Nanjing.

J. B. Keller. (1986) 'Impact with friction', *Journal of Applied Mechanical*, Vol. 53, pp.1-4.

Jin Niea, Jikuang Yang. (2014) 'A study of bicyclist kinematics and injuries based on reconstruction of passenger car–bicycle accident in China', *Accident Analysis and Prevention*, Vol. 71, pp. 50-59.

LiJun Xu. (2008) 'Numerical value analysis of multibody systems with unilateral constraint', *M.S. dissertation, Dalian University of Technology*, Dalian, China.

R. M. Brach. (1984) 'Friction, restitution, and energy loss in planar collisions', *ASME, Journal of Applied Mechanical*, Vol. 51, pp. 164-170.

The traffic accident Evidence Inspection (2005), *The people's Republic of China public security industry standard*s, GA41

Toor, A., Araszewski, M.(2003) 'Theoretical versus empirical solutions for vehicle pedestrian collisions', *SAE*, paper 2003-01-0883.

Wenli Yao, Bin Chen and Caishan Liu. (2005) 'Energetic coefficient of restitution for planar impact in multi-rigid-body system with friction', *International journal of impact engineering*, Vol.31, pp.255-265.

WenLi Yao, YuPing Wang, Li Bian, and Zhen Zhao. (2007) 'Progress in dynamics of impact and contact of multi-rigid-body systems', *Mechanics in Engineering*, Vol. 29, pp.9-12.

Xuejing Du, Jinpeng Li. (2013) 'Simulation of Pedestrian Colliding with Microbus Windshield', *Key Engineering Materials*, Vol. 572, pp.574-577.

XU Hongguo, REN You, DU Xuejing, LIU Fuju. (2013) 'A study on thrown object's kinetics of vehicle crash based on vehicle crash scatters', *Highlights of Science paper Online*, Vol. 6, pp.1119-1123.